Am J Transl Res 2019;11(9):5531-5545
www.ajtr.org /ISSN:1943-8141/AJTR0100318

Original Article

Xiaoyaosan prevents atherosclerotic vulnerable plaque formation through heat shock protein/glucocorticoid receptor axis-mediated mechanism

Wenjun Fu[1*], Mingtai Chen[2*], Lijun Ou[2], Tao Li[2], Xiao Chang[3], Ruolan Huang[3], Jian Zhang[4], Zhong Zhang[2]

[1]Centre for Integrative Medicine, School of Basic Medical Science, Guangzhou University of Chinese Medicine, Guangzhou 510006, Guangdong, China; Departments of [2]Cardiovascular, [3]Intensive Care Unit, Shenzhen Traditional Chinese Medicine Hospital, The Forth Clinical Medical College of Guangzhou University of Chinese Medicine, Shenzhen 518033, Guangdong, China; [4]Heart Failure Center, Fuwai Hospital Chinese Academy of Medical Sciences, Beijing 100037, China. [*]Equal contributors.

Received March 13, 2019; Accepted July 31, 2019; Epub September 15, 2019; Published September 30, 2019

Abstract: Atherosclerosis is a metabolic and chronic inflammatory disease caused by deposition of lipoproteins in arteries. However, the diagnostic drug and the mechanism for this vascular disease are less studied. In the present study, atherosclerosis model was developed using apolipoprotein E-deficient mice that was treated with long-term high-fat food and chronic stresses. Xiaoyaosan (XYS) and glucocorticoid receptor (GR) antagonist RU 38486 were orally administrated to the mice. The change of aortic root vessels was observed by histological analysis. The results indicate that high-fat food coupled with chronic stress induced atherosclerosis in mice model, with plaque formation in the entire aortas foam cells and macrophage infiltration in aortic tissues. However, XYS granules inhibited the development of atherosclerotic lesion, with down-regulation of GC, TC, TG, HDL-C, ox-LDL, LDL-C, IFN-γ, IL-6, IL-1β, and TNF-α measured by ELISA method; XYS inhibited the expressions of GR, CD36, HSP27/60/90, and induced ABCA1 in atherosclerotic mice, which was measured by qPCR and Western blot, which showed similar effect as positive control RU 38486 did. The interaction between HSP90-GR complexes and CD36 was validated in atherosclerotic mice. Our results inferred that the HSP/GR complex-mediated CD36 axis was involved in the regulation of atherosclerosis development in mice verified by Co-IP assay, EMSA, and Chip-PCR. These findings not only provide the potential therapeutic value of Xiaoyaosan for atherosclerotic vulnerable plaque but also brought forth a novel strategy for preventing the formation and treatment of atherosclerotic vulnerable plaques through the elucidated mechanism of XYS on vulnerable plaque.

Keywords: Atherosclerosis, vulnerable plaque, HSP/GR axis, xiaoyaosan formula

Introduction

Atherosclerosis is a metabolic and chronic inflammatory disease in arteries, especially in those with relatively larger size [1]. The deposition of lipoproteins, including the accumulation of low-density lipoprotein (LDL) and oxidized LDL (ox-LDL) at arterial intima, initiates reactive oxidative species (ROS) production, endothelial dysfunction, and the subsequent stimulation of atherosclerosis [1-4]. Along with the deposition of lipoproteins and dysfunction, lipoproteins were immoderately flowed into the intimal macrophage of the vascular wall [1, 4]. Foam cells and atherosclerotic plaques such as vulnerable plaques are formed accordingly [1].

Vulnerable plaque is the primary cause of approximately 70% of the acute myocardial infarction, thrombotic, and sudden coronary deaths, and thus the title 'Culprit Plaque' [5]. Vulnerable plaque is characterized by high level of lipid, low level of collagen, stenosis, low stability, macrophage density, active inflammation, and expansive remodeling [5]. It increases the risk of cardiovascular events [5-7]. Therefore, in the cardiovascular research, vulnerable plaque is considered as a critical factor in diagnosis and preventive therapies [8].

Previous studies have shown that the inflammatory activation of macrophages could reduce the stability of atherosclerotic plaques [9].

Glucocorticoids (GCs) contribute to the metabolic changes [10] and have been widely used as one of the most effective anti-inflammatory treatments [11]. GCs are endogenously expressed in response to inflammation and subsequently works as feedback inhibitor of the immune system [12]. The anti-inflammatory, proliferative, and migratory properties of GCs impelled its usage as potential inhibitors of atherosclerosis and restenosis [13]. However, there was an increase in cardiovascular risk owing to side effects of endothelial dysfunction and vasoconstriction [13]. In addition, substantial evidences show the association and interaction of heat-shock proteins (HSPs) with GCs and glucocorticoid receptor (GR) in bone formation, human cancer development, and immune diseases [14-17]. HSPs, such as HSP90, 60, 70, and 65, are associated with atherosclerosis, inflammatory responses, and atherosclerotic plaque formation [18-20]. It has been reported that HSP90 is necessary for the function of folding, trafficking, and steroid binding conformation of L cell GR [17, 21, 22].

The Xiaoyaosan (XYS) decoction is a kind of Chinese traditional prescription containing eight commonly used herbs, which has been extensively applied for the treatment of mental disorders including depression, for centuries in China [23, 24]. XYS decoction promotes the reduction in oxidative-stress-induced hippocampus neuron apoptosis [25]. It has been indicated that XYS decoction regulates changes in neuropeptide Y and leptin receptor in the arcuate nucleus of rat, after chronic immobilization stress (CIS), as well as reverses CIS-induced learning and memory deficit [26]. Recent studies revealed that XYS attenuated stress-induced anxiety behaviors by down-regulating the tumor necrosis fact (TNF)-alpha/JAK2-STAT3 pathway in the rat hippocampus [27]. However, the role of XYS on atherosclerosis development and its relevant mechanism remains elusive. This study aimed to investigate the potential effect of XYS on the regulation of atherosclerosis.

Materials and methods

Animals and model construction

Animal studies were conducted complying with the ARRIVE guidelines, with the approval of Local Ethical Committee (Guangzhou University of Chinese Medicine). Apolipoprotein E-deficient (*ApoE*$^{-/-}$) mice (n = 60, 6-8 weeks old, weight18-26 g. C57BL/6J background, strain B6.129P2-*Apoe*^{tm1}/Nju, #T001458) were purchased from Model Animal Research Center, Nanjing University, Nanjing, China. Before beginning the experiments, all mice were kept in rooms under controlled laboratory conditions (23-25°C, 12:12 h light-dark cycle, 50%-70% humidity) and fed with approved ordinary chow for at least 7 days along with free access to water. Fifty mice were randomly picked out and transferred to the controlled laboratory conditions as mentioned above, with given *ad libitum* access to ordinary chow and water. For model construction, 50 mice were intragastrically (ig) injected with 0.2 ml of high-fat emulsion (including 10% lard oil, 10% tween-80, 10% propylene glycol, 5% cholesterol, 1% Sodium cholate, 1% propylthiouracil, and 100% distilled water) daily and stimulated with chronic stressors (including ice water swimming for 30 s~60 s, day and night inversion for 24 h, fetter for 3 h, water deprivation for 24 h, and food deprivation for 24 h) with a frequency of a five-day cycle, for 60 days.

Experimental design

Ten mice in the control group were maintained under controlled laboratory conditions with the given *ad libitum* access to ordinary chow and water. The 50 mice treated with high-fat emulsion and stimulation were randomly divided into 5 groups (n = 10 in each group) and were treated with following strategies. Mice were daily administered with RU 38486 (Mifepristone; Sigma-Aldrich; Merck KGaA, Darmstadt, Germany; i.g, 25 mg/kg; n = 10), 5.256 g/kg (Low, n = 10; ig), 10.053 g/kg (Moderate, n = 10; ig) and 20.106 g/kg (High, n = 10; ig) and granule of Chinese herbal XYS formula, (Guangdong YifangPharmaceutical Co., Ltd. Foshan, China) for 60 days. Model control mice (n = 10) were daily administered with normal saline (ig) for 60 days. XYS granule formula consisted of 8 Chinese herbal medicines (9 g *Radix bupleuri*, 9 g *Angelica sinensis*, 9 g *Radix paeoniae alba*, 9 g *RhizomaAtractylodis*, 9 g *Poriacocos*, 4.5 g *Glycyrrhiza* root, 4.5 g *Menthahaplocalyx*, and 4.5 g dried ginger rhizome). Granules were immersed into distilled water and concentrated to 0.2 ml by boiling before administering it to mice. On the 60th day

of experimental design, all mice were killed by injecting a fatal dose of pentobarbital sodium (150 mg/kg, i.p.).

Enzyme-linked immunosorbent assay (ELISA)

Blood samples of mice were collected and centrifuged, and serum samples were prepared for enzyme-linked immunosorbent assay (ELISA). The content of serum GC, total cholesterol (TC), triacylglycerol (TG), high-density lipoprotein cholesterol (HDL-C), low-density lipoprotein cholesterol (LDL-C), ox-LDL, interferon (IFN)-γ, interleukin (IL)-6, IL-1β, and tumor necrosis factor (TNF)-α was detected using commercial ELISA kit according to manufacturer's instructions. ELISA kits for monitoring IFN-γ, IL-6, IL-1β, and TNF-α were obtained from Elabscience Biotechnology Co. Ltd. (Wuhan, China); GC was from Shanghai Enzyme-linked Biotechnology Co., Ltd (Shanghai, China); TC, TG, and HDL-C were from Nanjing Jiancheng Bioengineering Institute (Jiangsu, China); ox-LDL was from Xiamen Huijia Bioengineering Institute (Xiamen, China); and LDL-C was from Shanghai Yuanyan Bioscience Limited Company (Shanghai, China). A Thermo microplate reader (MultiskanMK3; Thermo Fisher Scientific Inc., Rockford, IL, USA) was used for the measurement of optical density (OD) at 450 nm.

Lesion and histology analysis

After anesthetization, whole aortas (from the heart to the iliac artery, n = 4 from each group) were perfused with cold PBS, dissected, and fixed in 4% paraformaldehyde overnight. For *en face* staining analysis, aorta trees were longitudinally excised and stained with 0.5% Oil Red O (Solarbio Science & Technology, Beijing, China) for 1 h. The aorta images were captured using a Leica stereoscope microscope (S8AP0; Leica, Wetzlar, Germany), and the percentage of Oil Red O-positive lesion surface areas in relation to the total surface area was determined using Image J software (https://imagej.nih.gov/nih-image).

For histology analysis, aortic root vessels were cut from isolated aortas (n = 3 from each group), fixed in 4% paraformaldehyde overnight, and frozen in optimal cutting temperature (OCT) compound (Sakura Finetek, Torrance, CA, USA), and cut into serial sections (10 μm in thickness) using a Leica cryotome (CM 1510 S, Leica). Three transverse sections, with 30 μm intervals, were stained with 0.3% Oil Red O working solution (Sigma-Aldrich; Merck KGaA) for lipid content in plaque area and hematoxylin staining solution (Sigma-Aldrich; Merck KGaA) for histopathology analysis.

Immunohistochemistry and immunofluorescence

To detect the expression of GR, CD36, and ATP-binding cassete A1 (ABCA1) in aortic root vessels, serial sections (10 μm in thickness) were immunohistochemically stained with anti-mouse antibody GR (1:200; Cell Signaling Technology, CST, Danvers, MA, USA), CD36 (1:300; Abcam, Cambridge, MA, USA), and ABCA1 (1:300; Abcam) at 4°C overnight. Corresponding HRP-conjugated secondary antibodies (anti-IgG, 1:10,000) were used. Histological scores (4-point scale: 0, 0%; 1, 0~25%; 2, 25%~75%; 3, > 75%) of tissues expressing GR, CD36, and ABCA1 were evaluated using a double-blind scoring method. For immunofluorescence analysis, sections were examined using primary antibodies and Alexa555-conjugated secondary antibody (1:1,500; Invitrogen Life Technologies, Carlsbad, CA, USA). DAPI (Invitrogen) was used to counter stain the nuclei. Examination was performed using laser-scanning confocal microscope (TCS-SP5, Leica). Fluorescent intensity was analyzed using Image J software.

Western blot analysis

Western blot was performed to detect the expression of related proteins using standard protocols. Cytoplasmic and nuclear proteins were extracted from aortic root vessels using a nuclear/cytoplasmic protein extraction kit (P0028; Beyotime Institute of Biotechnology, Guangzhou, China) following the manufacturer's instructions. Protein concentrations were determined using a Bradford protein assay kit (Thermo Fisher Scientific Inc.). About 10% SDS-PAGE (Shanghai Sangon Biological Engineering Technological Co. Ltd., Shanghai, China) and Millipore PVDF membranes (Millipore, Billerica, MA, USA) were used for protein separation and immunoblotting analysis. Bovineserum albumin (BSA, 5% in TBST; Amresco, Solon, OH, USA; FA016-50G) was used for membrane block. Immunoblotting analysis was performed using specific primary antibodies, including

Table 1. The primer or probe sequences used in our study

Gene	Primers	Sequence (5'-3')
β-actin	Forward	CATTGCTGACAGGATGCAGA
	Reverse	CTGCTGGAAGGTGGACAGTGA
GR	Forward	ACAGTCAAGGTTTCTGCGTCT
	Reverse	TCCCCATCACTTTTGTTTCG
CD36	Forward	ATGGGCTGTGATCGGAACTG
	Reverse	TTTGCCACGTCATCTGGGTTT
ABCA1	Forward	TGTGACCAGAGGGGATGCG
	Reverse	CAACCTTGCCAACTTCCTTTTC
HSP27	Forward	CCCACCCTCTATCACGGCTA
	Reverse	ATCTGGGGTAAAGTGGCTCAC
HSP60	Forward	CACAGTCCTTCGCCAGATGAG

anti-GR (1:300; CST), anti-ABCA1 (1:1,000; Abcam), anti-CD36 (1:8,000; Abcam), anti-HSP60 (1:4,000; Abcam), anti-HSP27 (1:2,000; CST), anti-HSP90 (1:20,000; CST), anti-GAPDH (1:10,000; Shanghai Kangcheng Biotechnology Co. LTD., Shanghai, China), and HRP-conjugated secondary antibody (anti-rabbit IgG, 1:20,000; Boster, Wuhan, China), respectively. Enhanced chemiluminescence detection kit (Millipore) was used for the visualization of membranes with Image-Pro Plus 6.0 software (Media Cybernetics Inc., Bethesda, MD, USA).

Quantitative real-time PCR

The relative mRNA expression level of the genes studied was detected using quantitative real-time PCR (qRT-PCR). Extraction of total RNA was performed using TRIzol reagent (TaKaRa, Tokyo, Japan), and separation of cytoplasmic and nuclear RNA was conducted using PARIS™ Kit (Invitrogen) according to the manufacturer's instruction. The synthesis of the first-strand cDNA was implemented using Bestar® qPCR RT Kit (DBI Bioscience, Shanghai, China). The relative mRNA expression levels of GR (total, cytoplasmic and nuclear), ABCA1, CD36, HSP60, HSP27, and HSP90 were determined using a Bestar® Sybr Green qPCR master mix (DBI Bioscience) using the primers listed in **Table 1**. An Agilent Stratagene Mx3000P RT-PCR machine (Agilent, California, CA) was used for the amplification according to standard procedures (Initial denaturation at 94°C for 2 min; followed with 40 cycles of 94°C for 20 s, 58°C for 20 s, and 72°C for 20 s). The relative expression levels of gene mRNAs were computed using the $2^{-\Delta\Delta Ct}$ methods. The β-actin gene was used as the internal reference gene.

Co-immunoprecipitation (Co-IP) assay

The interaction between HSP90 and GR proteins was identified using Co-IP assay by a Pierce® Co-IP Kit (Thermo Scientific Inc.). HSP-90 or GR antibody were incorporated with resin in a spin column at 4°C for 2 h. Cytoplasmic protein lysates were isolated as mentioned above and immunoprecipitated with anti-HSP90/GR antibody in column at 4°C overnight, with gentle rotation. The combined protein samples were eluted and quantified using Bradford protein assay kit (Thermo Fisher Scientific Inc.), and stored at -80°C. Protein interaction was identified using Western blot analysis with anti-HSP90/GR antibody. All reactions were performed in triplicate.

Electrophoretic mobility shift assay (EMSA)

The nuclear protein lysates were obtained and quantified using the aforementioned methods. EMSA was implemented using a LightShift® Chemiluminescent EMSA Kit (Thermo Fisher Scientific Inc.) according to the manufacturer's instruction. In brief, prepared probes, including biotin-labeled, cold , and mutant probes, were diluted (1:100, in ddH_2O) and added into reaction mixture containing 5-μg nucleoprotein. Before chromogenic reaction electrophoresis onto 6.5% polyacrylamide (Genview, Beijing, China) and transformation onto PVDF membrane (Millipore) was implemented and scanned using a Microtek Bio-5000 scanner (Microtek Lab, Inc., Santa Fe Springs, CA). Analysis was conducted using Image-Pro Plus 6.0 software (Media Cybernetics Inc., Bethesda, MD, USA). All reactions were performed in triplicates.

Chromatin-immunoprecipitation (ChIP)

ChIP assay coupled with quantitative PCR (ChIP-qPCR) was conducted to confirm the DNA-binding ability of GR using a Simple ChIP Plus Enzymatic Chromatin IP Kit (CST)., Aortic tissues were treated with protease inhibitor cocktail coupled with gradually decreased formaldehyde (37%~1.5%) at room temperature for 20 min to cross-link chromatin according to the manufacturer's protocol, which was then inhibited by glycine solution at room temperature for 5 min. Cross-linked chromatins

were broken down into DNA fragments (200 bp in length) by digestion with DNA micrococcal nuclease at 37°C for 20 min and sonication (15 s) for 20 times. ChIP reaction was performed using 5 μg of anti-GR antibody or IgG (Negative control) enriched in protein G magnetic beads (Invitrogen) at 4°C overnight. The immunoprecipitated complexes were then eluted using ChIP elution buffer at 65°C for 30 min, and DNA were de-crosslinked from proteins using proteinase K (CST) at 65°C for 2 h. The obtained DNA samples were purified and subjected to PCR analysis and 2% agarose gel (Biowest, Nuaillé, France). All reactions were performed in triplicate.

Statistical analysis

Statistical analysis was performed using GraphPad Prism 6.0 (GraphPad Software, San Diego, CA, USA). All data were expressed as mean ± SD. Unpaired Student's t-test and two-way ANOVA was used to analyze different levels between two groups and more than three groups, respectively. Unpaired Student's t-test was used to analyze lipid accumulation, atherosclerotic lesion, and aortic roots in aortas; two-way ANOVA was used to analyze the contents of GC and parameters related to lipid, the expression of GR, CD36, and ABCA1. $P < 0.05$ was considered statistically significant.

Results

XYS granules inhibit development of atherosclerotic lesion

The model of atherosclerotic mice maintained on high-fat emulsion and chronic stresses for 60 days developed a significant atherosclerotic lesion in aortas. *En face* staining analysis showed the plaque formation in entire aortas (**Figure 1A**), and histology analysis showed the obvious accumulation of Oil red O-positive staining and foam cells (**Figure 1B**) and macrophage infiltration in aortic tissues (**Figure 1C**) compared to that of *ApoE*$^{-/-}$ mice from normal control group, indicating the formation of atherosclerosis vulnerable plaques in the model mice fed with high-fat food coupled with induced chronic stress. However, plaque formation and macrophage infiltration were remarkably decreased in mice administered with XYS granules and GR inhibitor RU 38486 compared with the model mice.

XYS granules control the profiles of serum biochemical indexes

ELISA was performed to analyze the profiles of serum biochemical indexes. The contents of GC, TC, TG, HDL-C, ox-LDL, and LDL-C in atherosclerosis model were significantly increased compared to those in control mice ($P < 0.05$, **Figure 2A**). On contrast, intragastric administered XYS granules reduced the contents of all serum biochemical indexes in a dose-dependent manner. Atherosclerotic *ApoE*$^{-/-}$ mice treated with high-dose XYS granules (20.106 g/kg per day) showed the lowest levels of serum biochemical indexes, although higher than those in positive control and RU 38486-treated mice ($P < 0.05$, **Figure 2A**). Similar trends were observed in serum cytokines IFN-γ, IL-6, IL-1β, and TNF-α (**Figure 2B**). These analyses proved that administration of XYS granules prevented the development of atherosclerosis in mice and provided an anti-inflammatory effect.

XYS granules suppress GR and CD36 enhances ABCA1 in atherosclerotic mice

It was observed statistically that the administration of XYS granules increased cytoplasmic GR and decreased nuclear GR in atherosclerotic mice in a dose-dependent manner, respectively ($P < 0.05$, **Figure 3A**). Moreover, it significantly decreased CD36 expression and induced ABCA1 level in atherosclerotic *ApoE*$^{-/-}$ mice ($P < 0.001$). The protein patterns of GR, CD36, and ABCA1 were perfectly duplicated similar to that of mRNA levels (**Figures 3B** and **4**).

XYS granules prevent HSP27/60/90 in atherosclerotic mice

The results revealed the inhibitory effect of XYS granules on the expression of HSP27, 60, and 90. Increased expression of HSP27, 60 and 90 mRNA, and protein was observed in atherosclerotic *ApoE*$^{-/-}$ mice compared to the control ($P < 0.001$, **Figure 5A** and **5B**), whereas XYS granules (20.106 g/kg per day) and RU 38486 administration impeded the levels of HSP27/60/90. These results imply that XYS granules might have attenuated the HSP-mediated signaling in aortic vessels in atherosclerotic mice.

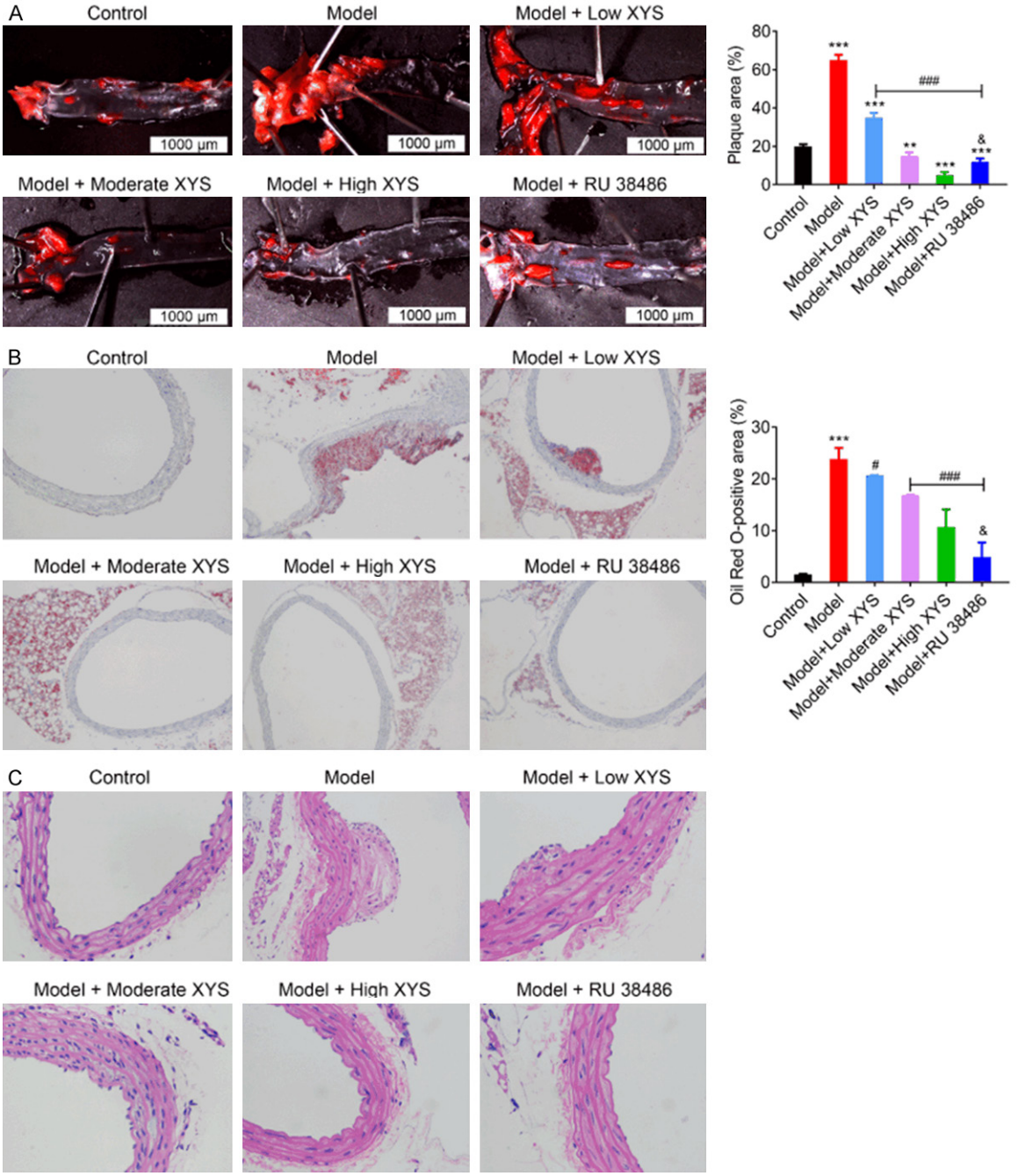

Figure 1. XYS granules inhibit the formation of atherosclerotic plaque. Atherosclerotic *ApoE*$^{-/-}$ mice model was induced by high-fat emulsion and chronic stresses for 60 days and treated with low, moderate, high XYS and RU 38486, respectively. A. The en face analysis using Oil red O staining and plaque area (%) analysis for atherosclerotic lesion in aortas in different groups. B. Oil red O staining for lipid accumulation and Oil red O-positive area (%) analysis in aortic roots in different groups (magnification × 200). C. Hematoxylin and eosin (H&E) staining for aortic roots in different groups (magnification × 400). Data shown are means ± SD. ** and ***, $P < 0.01$ and $P < 0.001$ vs. control, respectively. # and ###, $P < 0.05$ and $P < 0.001$ vs. model, respectively. &, $P < 0.05$ vs. Model + high XYS.

XYS granules promote HSP90 interaction with GR and CD36

Our CoIP data illustrated the significant interaction between HSP90 and GR in model mice (**Figure 6A**). EMSA and ChIP's result further implicated the binding of GR to CD36 promoter, suggesting the interaction between HSP90-GR complexes and CD36, especially in the atherosclerotic mice (**Figure 6B** and **6C**).

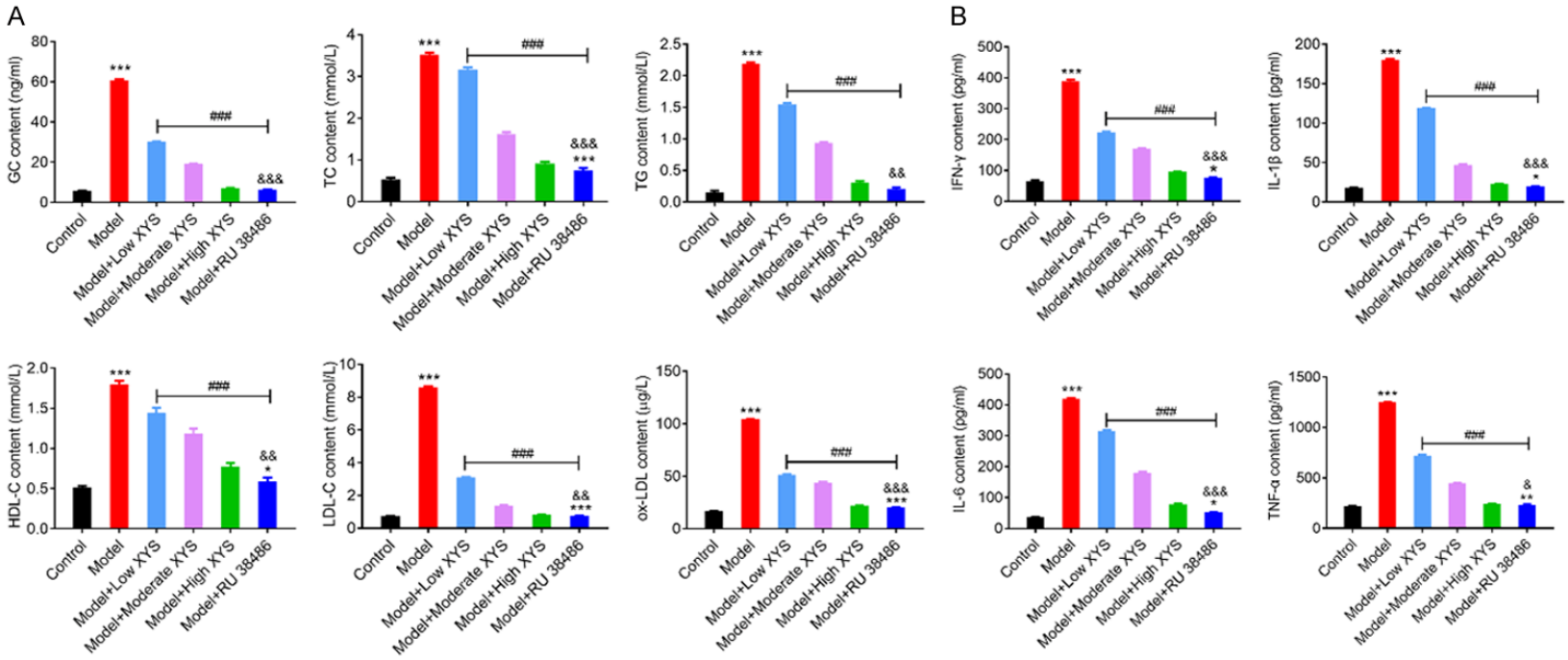

Figure 2. Administration of XYS granules prevented the development of atherosclerosis in mice and presented anti-inflammatory effect. A. The contents of GC and parameters related to lipid in different groups, including GC, TC, TG, HDL-C, ox-LDL, and LDL-C. B. The contents of serum cytokines in different groups, including IFN-γ, IL-6, IL-1β, and TNF-α. All the indexes were detected using ELISA. Data shown are means ± SD. ***, $P < 0.001$ vs. control. ###$P < 0.001$ vs. model. &, &&, and &&& $P < 0.05$, $P < 0.01$, and $P < 0.001$, vs. model + high XYS, respectively.

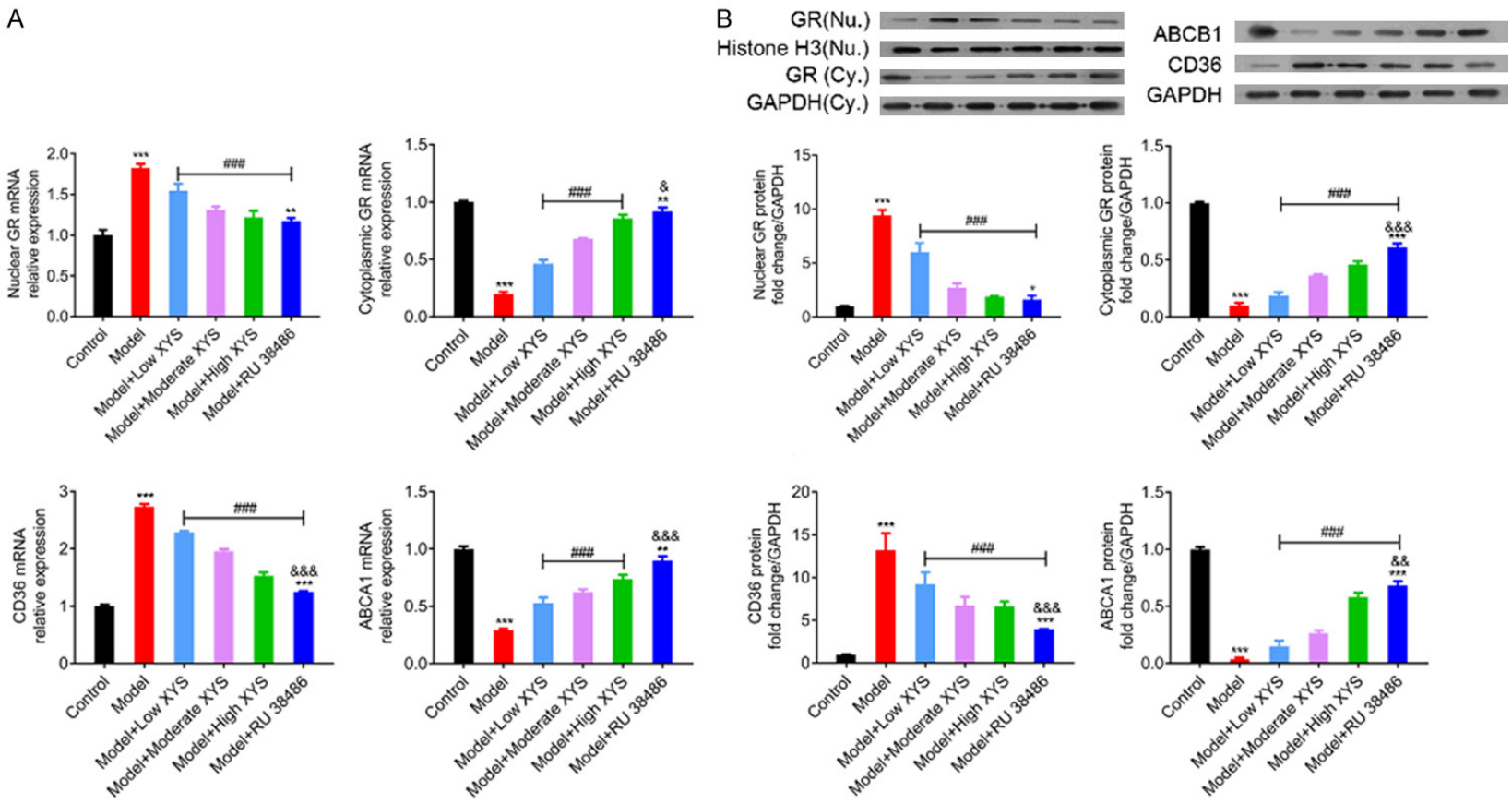

Figure 3. XYS granules suppress GR and CD36 enhances ABCA1 in atherosclerotic mice. A. The mRNA relative expression level analysis of GR, CD36, and ABCA1 gene in different groups was detected using qRT-PCR. B. The protein expression level of GR, CD36, and ABCA1 protein was determined using Western blot analysis. GAPDH act as an internal standard. Data shown are means ± SD. *, ** and ***, $P < 0.05$, $P < 0.01$ and $P < 0.001$ vs. control, respectively. ###$P < 0.001$ vs. model. &, && and &&&, $P < 0.05$, $P < 0.01$, and $P < 0.001$ vs. model + high XYS, respectively.

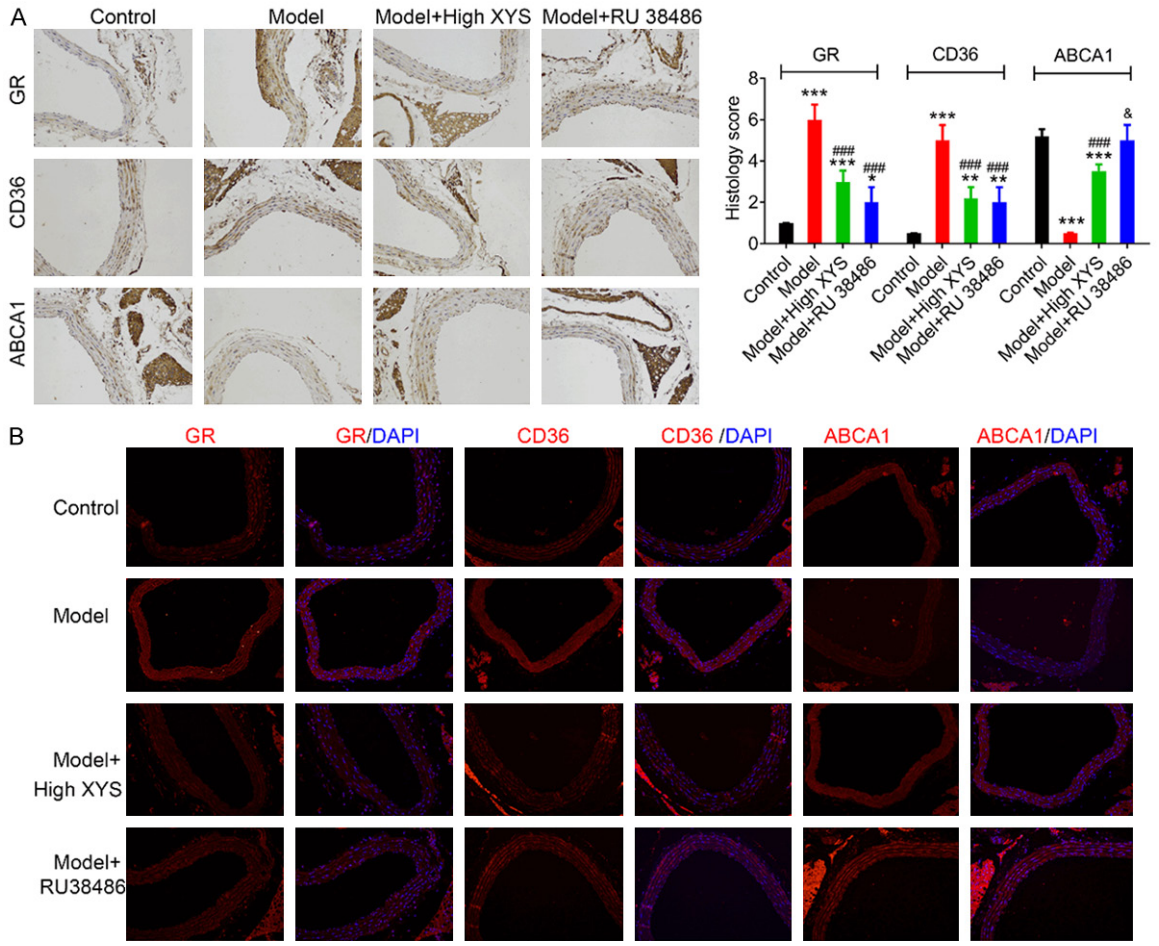

Figure 4. The expression of GR, CD36, and ABCA1 protein in aortic root vessels analyzed by immunohistochemistry and immunofluorescence, respectively. A. The expression of GR, CD36, and ABCA1 protein in aortic root vessels measured by immunohistochemistry in different groups. Histology scores were the sums of nuclear and cytoplasmic scores by double blind scoring method. B. The expression of GR, CD36, and ABCA1 protein in aortic root vessels measured by immunofluorescence analysis in different groups. The secondary antibody was conjugated with Alexa 555 (red). Nucleus was stained with DAPI (Blue). Magnification, x 200. Data shown are means ± SD. *, ** and ***, $P < 0.05$, $P < 0.01$ and $P < 0.001$ vs. control, respectively. ###$P < 0.001$ vs. model. &$P < 0.05$ vs. model + high XYS.

Discussion

There are substantial evidence showing the association and interaction of HSPs with GR in immune diseases, and HSP90 is necessary for the GR function [17, 21, 22]. In our study, we have demonstrated the correlation of HSP90, 60, and 27 with GR and GC profiles in high-fat food combined with chronic stresses-induced atherosclerotic *ApoE*$^{-/-}$ mice. We have also confirmed their association with macrophage CD36 and ABCA1. However, the administration of traditional Chinese medicine (TCM) XYS formula decoction and GR inhibitor RU 38486 suppressed these changes and atherosclerotic development.

High-fat food-induced metabolic disorders promote lipoproteins' accumulation, oxidative stresses, and active inflammation in macrophages of the vascular wall and result in the formation of atherosclerotic plaques (**Figure 7**) [1, 4]. In the similar scenario, our present study found the atherosclerotic histological changes in model mice, combined with obviously increased cholesterol and lipid parameters (including GC, TC, TG, HDL-C, LDL-C, and ox-LDL) and elevated release of serum inflammatory molecules (including IFN-γ, IL-6, IL-1β, and TNF-α). These suggested that high-fat food combined with chronic stresses successfully induced atherosclerosis in our present study. The anti-inflammatory, -proliferative, and

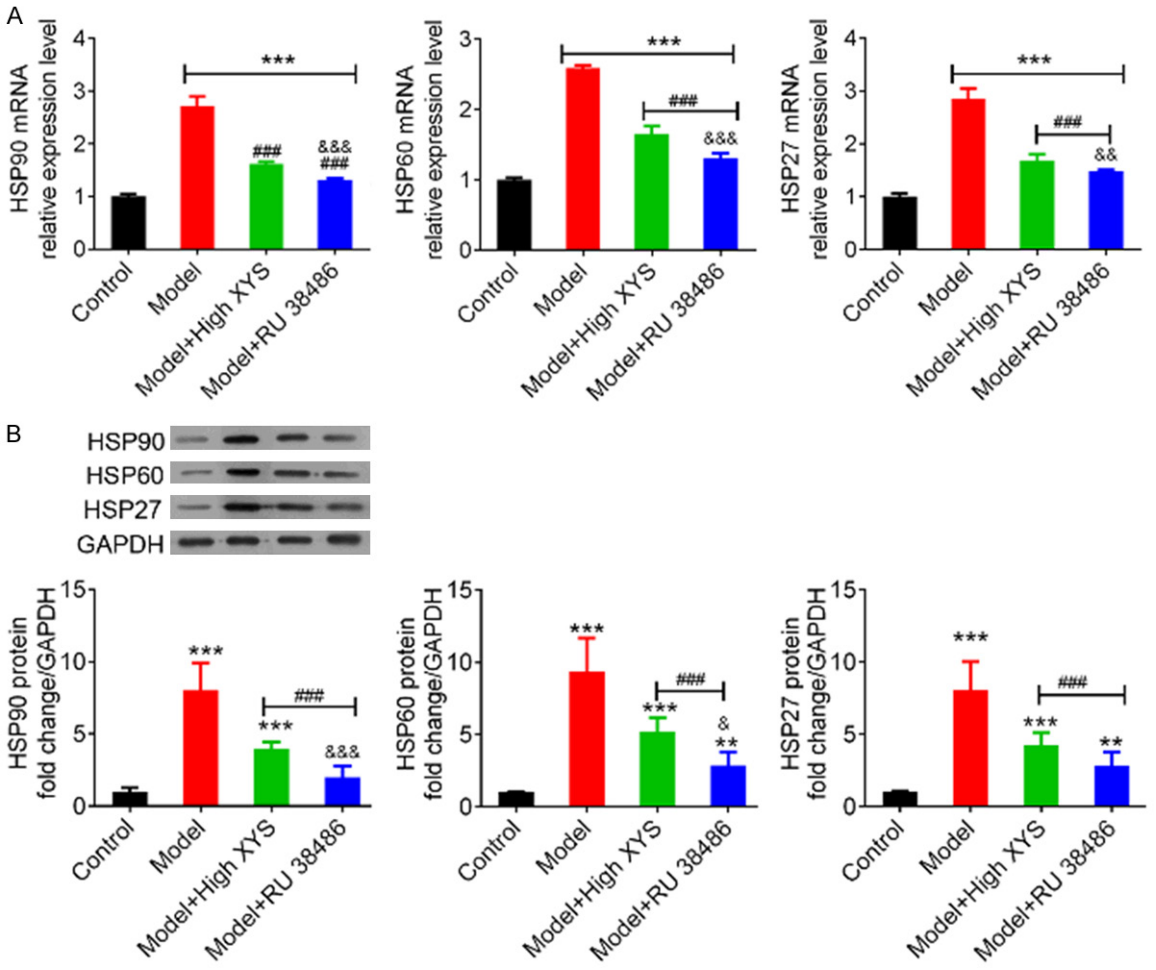

Figure 5. XYS granules prevent the expression of HSP. A. The mRNA relative expression level of HSP27, HSP60, and HSP90 measured by qRT-PCR. B. The protein expression change of HSP27, HSP60, and HSP90 analyzed by Western blot. The protein bands were analyzed using Image J software. GAPDH act as an internal standard. Data shown are means ± SD. ** and ***, $P < 0.01$ and $P < 0.001$ vs. control, respectively. ###$P < 0.001$ vs. model. &, &&, and &&& notes $P < 0.05$, $P < 0.01$, and $P < 0.001$ vs. model + high XYS, respectively.

-migratory properties of GCs prevent atherosclerosis, whereas the endothelial dysfunction and vaso-constriction increased the risk of cardiovascular events [13]. XYS alleviates the atherosclerotic damages as well as inflammation in mice model, which exerts protective function on ILs/TNF-α-GC/GR feedback regarding oxidative stress and inflammation in atherosclerotic *ApoE*$^{-/-}$ mice.

GR is a nuclear transcription factor. GC-induced TNF receptor (GITR) family-related protein has been identified as a member of the TNF receptor superfamily (TNFRSF18). The stimulation of GITR has been reported to induce the activation of matrix metalloproteinase-9 (MMP9) and production of pro-inflammatory cytokines in lipid-rich macrophage cells [9]. Notably, XYS suppresses TNF-alpha/JAK2-STAT3 pathway in the hippocampus [27]. In addition, Kol *et al* showed the macrophage TNF-α and MMPs expression could be regulated by HSPs in atheroma [28]. Accumulative evidence unraveled the interaction of HSPs with GR [14-17], except for the association of HSPs with atherosclerosis, inflammatory responses, and atherosclerotic plaque formation [18-20]. Consistently, we have demonstrated the interaction of HSP90 with GR by CoIP assay, suggesting the vital roles of GR in atherosclerosis development by regulating GC content, HSP/MMP activation, and plaque vulnerability (**Figure 7**).

Previous report had shown that HSPs accelerated atherosclerosis via down-regulating the

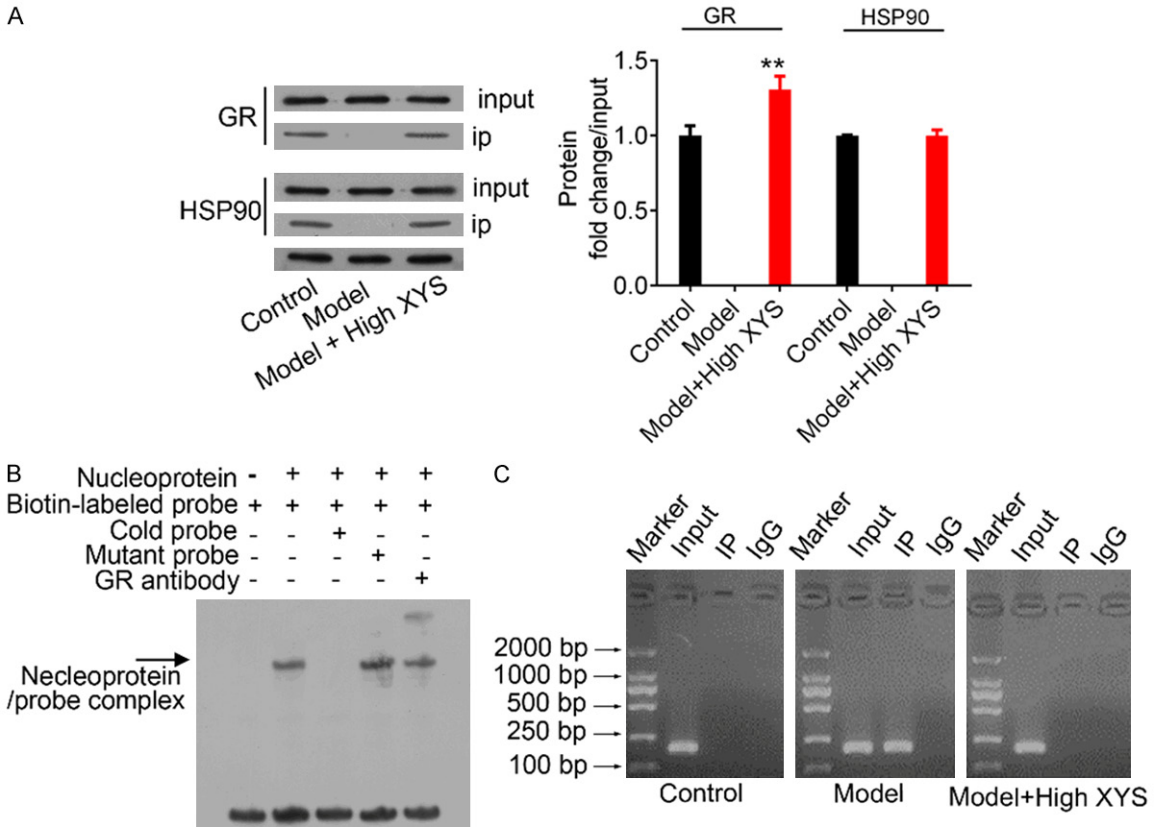

Figure 6. XYS granules promote HSP90 interaction with GR and CD36. The immunoprecipitation and electrophoretic mobility shift assays. A. Co-immunoprecipitation (Co-IP) assay for GR and HSP90 proteins. HSP90 or GR antibody were incorporated with resin in a spin column at 4°C for 2 h. Cytoplasmic protein lysates were isolated as above and immunoprecipitated with anti-HSP90/GR antibody in column at 4°C overnight, with gentle rotation. Protein interaction was detected using Western blot analysis as above with anti-HSP90/GR antibody. All reactions were performed in triplicate. Upside, HSP90 co immunoprecipitates with GR. Below, GR co immunoprecipitates with HSP90. B. The electrophoretic mobility shift (EMSA) assay for the binding of GR to *CD36* promoter. Biotin-labeled probes, cold probes, and mutant probes were diluted (1:100, in ddH_2O) and added into reaction mixture containing 5-μg nucleoprotein. Electrophoresis onto 6.5% polyacrylamide and transformation onto PVDF membrane was implemented before chromogenic reaction and scanning using a Microtek Bio-5000 scanner. Analysis was conducted using Image-Pro Plus 6.0 software. All reactions were performed in triplicates. C. Chromatin-immunoprecipitation (ChIP) assay for GR encoding DNA with *CD36* promoter. ChIP reaction was performed using 5 μg of anti-GR antibody or IgG (Negative control) enriched in protein G magnetic beads (Invitrogen) at 4°C overnight. The immunoprecipitated complexes were then eluted using ChIP elution buffer at 65°C for 30 min and DNA were de-crosslinked from proteins using proteinase K (CST) at 65°C for 2 h. The obtained DNA samples were purified and subjected to PCR analysis and 2% agarose gel. All reactions were performed in triplicate. Data shown are means ± SD (n = 3). **Indicates $P < 0.01$ vs. control.

expression of ABCA1 [29]. The knockdown of ABCA1 promoted atherosclerotic lesion formation [30, 31]. Another atherosclerosis contributor is CD36 expression. CD36 is a scavenger receptor expressed in macrophages, and a new identified cell surface receptor for HSPs [32-34], and a proteolytically degradable substrate of matrix-degrading enzyme MMP9 [35, 36]. Ox-LDL-bound CD36 promotes atherosclerosis [37, 38]. CD36 and ABCA1 are cholesterol transporters that are involved in cholesterol efflux in macrophages [31]. In our present study, we demonstrated the elevated ox-LDL, HSPs and CD36, as well as down-regulated ABCA1 in atherosclerotic *ApoE*$^{-/-}$ mice, suggesting the important roles of the ox-LDL/CD36/HSP-ABCA1 axis in atherosclerosis. In addition, we also detected the binding of nuclear transcription factor GR to CD36 promoter using EMSA and ChIP assays. These demonstrated the vital roles of HSP/GR complex-mediated CD36 axis in atherosclerosis development.

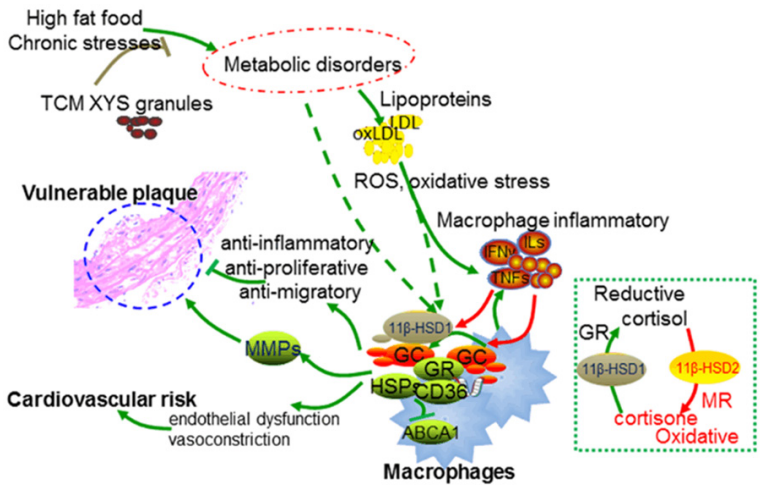

Figure 7. The potential mechanism associated with HPS/GR axis-mediated plaque formation. High-fat food-induced metabolic disorders promote lipoproteins accumulation, oxidative stresses, and active inflammation in macrophage of the vascular wall and accordingly result in the formation of atherosclerotic plaques by affecting the expression of GC, GR, HSP, CD36, and ABCA1. Xiaoyaosan prevents atherosclerotic vulnerable plaque formation through regulating the expression of heat shock protein, glucocorticoid receptor, and CD36 axis. Pathways in the right green box indicate the conversion between cortisol and cortisone, red and black part notes the oxidative 11β-HSD2 activity (cortisol-cortisone conversion) and reductive 11β-HSD1 activity (cortisone-cortisol conversion), respectively. Different colors of lines and notes do not have specific meanings.

XYS granule formula contains 8 kinds of Chinese herbal medicines (9 g Radix bupleuri, 9 g Angelica sinensis, 9 g Radix paeoniae alba, 9 g Rhizoma Atractylodis, 9 g Poriacocos, 4.5 g Glycyrrhiza root, 4.5 g Menthahaplocalyx, and 4.5 g dried Ginger rhizome). Recent finding indicated that the compound Saikosaponin D (SSD) from Radix Bupleuri interacted with beta-catenin via hydrogen bonds and hydrophobic interaction and suppressed triple-negative breast cancer cell growth [39]. It significantly improved cell viability and inhibits the elevation of TNF-alpha, IL-1beta, and IL-6, which was in line with our finding with XYS [40]. *Angelica sinensis* (oliv.) diels water extract contributes to anti-inflammatory effects on raw 264.7 induced with lipopolysaccharide via NO-bursting/calcium-mediated JAK-STAT pathway and it [41]. Notably, *Poriacocos* polysaccharides presented antihepatotoxic benefits on acetaminophen-lesioned livers through suppressing cell death, reducing hepatocellular inflammatory stress and Hsp90 bioactivity, while roots and rhizomes of *Glycyrrhizauralensis* Fisch. (Fabaceae) exerted inhibitory function toward the phosphorylation of heat shock protein 27, which were in agreement with our finding regarding the XYS in mediating of HSP and inflammation [42, 43]. The therapeutic roles of a TCM formula of XYS were elucidated on balancing metabolisms of lipid, energy, and inflammatory factors [44, 45]. The effective treatments of XYS formula had been proved in diabetes, depression, anxiety, polycystic ovary, and hepatic fibrosis [46-49]. However, the exact active ingredients of XYS on atherosclerosis, such as certain kinds of polysaccharides, need to be further identified, and the molecular mechanisms of the compounds are to be investigated.

Conclusions

In summary, we confirmed the long-term high-fat food coupled with chronic stresses (60 days) induced atherosclerotic *ApoE*$^{-/-}$ mice. Within this model, TCM XYS granules suggest potential clinical value on the treatment of atherosclerosis through regulating HSP90/60/27, GR, CD36, and ABCA1.

Acknowledgements

This work was supported by National Natural Science foundation of China (No. 81573922) and Sanming Project of Medicine in Shenzhen (No. SZSM201612033).

Disclosure of conflict of interest

None.

Abbreviations

XYS, Xiaoyaosan; TNF-α, tumor necrosis factor; TCM, Traditional Chinese medicine; ABCA1, ATP-binding cassete A1; GC, glucocorticoid; ROS, reactive oxidative species; TC, total cholesterol; HSPs, heat-shock proteins; HDL-C, high-density lipoprotein cholesterol; GR, glucocorticoid receptor; LDL-C, low-density lipoprotein cholesterol; CIS, chronic immobilization stress; IFN-γ, interferon-γ; ig, intragastrically.

Address correspondence to: Dr. Jian Zhang, Heart Failure Center, Fuwai Hospital Chinese Academy of Medical Sciences, No. 167 North Lishi Road, Xicheng District, Beijing 100037, China. Tel: +86 010-68314466; E-mail: fuwaixinshuai@163.com; Dr. Zhong Zhang, Department of Cardiovascular, Shenzhen Traditional Chinese Medicine Hospital, The Forth Clinical Medical College of Guangzhou University of Chinese Medicine, Fuhua Street, Futian District, Shenzhen 518033, Guangdong, China. Tel: +86 755-88607540; E-mail: 179080693@qq.com; zhangzhong201608@163.com

References

[1] Shen D, Bo W, Wen L, Wang L, Song X, Guo C, Li Y, Liu F, Zhu F and Wang Q. Systemic application of 3-methyladenine markedly inhibited atherosclerotic lesion in ApoE-/- mice by modulating autophagy, foam cell formation and immune-negative molecules. Cell Death Dis 2016; 7: e2498.

[2] Witztum JL. The oxidation hypothesis of atherosclerosis. Lancet 1994; 344: 793-795.

[3] Li H, Horke S and Förstermann U. Vascular oxidative stress, nitric oxide and atherosclerosis. Atherosclerosis 2014; 237: 208-219.

[4] Nomura J, Busso N, Ives A, Matsui C, Tsujimoto S, Shirakura T, Tamura M, Kobayashi T, So A and Yamanaka Y. Xanthine oxidase inhibition by febuxostat attenuates experimental atherosclerosis in mice. Sci Rep 2014; 4: 4554.

[5] Naghavi M, Libby P, Falk E, Casscells SW, Litovsky S, Rumberger J, Badimon JJ, Stefanadis C, Moreno P, Pasterkamp G, Fayad Z, Stone PH, Waxman S, Raggi P, Madjid M, Zarrabi A, Burke A, Yuan C, Fitzgerald PJ, Siscovick DS, de Korte CL, Aikawa M, Juhani Airaksinen KE, Assmann G, Becker CR, Chesebro JH, Farb A, Galis ZS, Jackson C, Jang IK, Koenig W, Lodder RA, March K, Demirovic J, Navab M, Priori SG, Rekhter MD, Bahr R, Grundy SM, Mehran R, Colombo A, Boerwinkle E, Ballantyne C, Insull W Jr, Schwartz RS, Vogel R, Serruys PW, Hansson GK, Faxon DP, Kaul S, Drexler H, Greenland P, Muller JE, Virmani R, Ridker PM, Zipes DP, Shah PK, Willerson JT. From vulnerable plaque to vulnerable patient a call for new definitions and risk assessment strategies: part I. Circulation 2003; 108: 1664-1672.

[6] De RR, Vasa-Nicotera M, Leistner DM, Reis SM, Thome CE, Boeckel JN, Fichtlscherer S and Zeiher AM. Coronary atherosclerotic plaque characteristics and cardiovascular risk factors-insights from an optical coherence tomography study. Circ J 2017; 81: 1165-1173.

[7] Arbabzadeh A and Fuster V. The myth of the "vulnerable plaque": transitioning from a focus on individual lesions to atherosclerotic disease burden for coronary artery disease risk assessment. J Am Coll Cardiol 2015; 65: 846-855.

[8] Bellinge JW, Francis RJ, Majeed K, Watts GF and Schultz CJ. In search of the vulnerable patient or the vulnerable plaque: (18)F-sodium fluoride positron emission tomography for cardiovascular risk stratification. J Nucl Cardiol 2018; 25: 1774-1783.

[9] Kim WJ, Bae EM, Kang YJ, Bae HU, Hong SH, Lee JY, Park JE, Kwon BS, Suk K, Lee WH. Glucocorticoid-induced tumour necrosis factor receptor family related protein (GITR) mediates inflammatory activation of macrophages that can destabilize atherosclerotic plaques. Immunology 2006; 119: 421-9.

[10] Ukkola O, Rosmond R, Tremblay A and Bouchard C. Glucocorticoid receptor Bcl I variant is associated with an increased atherogenic profile in response to long-term overfeeding. Atherosclerosis 2001; 157: 221-224.

[11] Barnes PJ and Adcock IM. Glucocorticoid resistance in inflammatory diseases. Lancet 2009; 373: 1905-1917.

[12] Morand EF, Leech M and Bernhagen J. MIF: a new cytokine link between rheumatoid arthritis and atherosclerosis. Nat Rev Drug Discov 2006; 5: 399-410.

[13] Hadoke PW, Iqbal J, Walker BR. Therapeutic manipulation of glucocorticoid metabolism in cardiovascular disease. Br J Pharmacol 2009; 156: 689-712.

[14] Mouradian M, Ma IV, Vicente ED, Kikawa KD and Pardini RS. Docosahexaenoic acid-mediated inhibition of heat shock protein 90-p23 chaperone complex and downstream client proteins in lung and breast cancer. Nutr Cancer 2017; 69: 92-104.

[15] Chen H, Xing J, Hu X, Chen L, Lv H, Xu C, Hong D and Wu X. Inhibition of heat shock protein 90 rescues glucocorticoid-induced bone loss through enhancing bone formation. J Steroid Biochem Mol Biol 2017; 171: 236-246.

[16] Vardas K, Ilia S, Sertedaki A, Charmandari E, Briassouli E, Goukos D, Apostolou K, Psarra K, Botoula E and Tsagarakis S. Increased glucocorticoid receptor expression in sepsis is related to heat shock proteins, cytokines, and cortisol and is associated with increased mortality. Intensive Care Med Exp 2017; 5: 10.

[17] Bresnick EH, Dalman FC, Sanchez ER and Pratt WB. Evidence that the 90-kDa heat shock protein is necessary for the steroid binding conformation of the L cell glucocorticoid receptor. J Biol Chem 1989; 264: 4992-7.

[18] Mu H, Wang L and Zhao L. HSP90 inhibition suppresses inflammatory response and reduc-

es carotid atherosclerotic plaque formation in ApoE mice. Cardiovasc Ther 2017; 35.
[19] Galović R, Flegar-Meštrić Z, Vidjak V, Matokanović M and Barišić K. Heat shock protein 70 and antibodies to heat shock protein 60 are associated with cerebrovascular atherosclerosis. Clin Biochem 2016; 49: 66-9.
[20] Lin SZ, Crawford TC and Mandal K. Role of heat shock proteins in atherosclerosis and atrial fibrillation. Current Immunology Reviews 2017; 13: 71-81.
[21] Pratt WB. The role of heat shock proteins in regulating the function, folding, and trafficking of the glucocorticoid receptor. J Biol Chem 1993; 268: 21455-8.
[22] Kojika S, Sugita K, Inukai T, Saito M, Iijima K, Tezuka T, Goi K, Shiraishi K, Mori T and Okazaki T. Mechanisms of glucocorticoid resistance in human leukemic cells: implication of abnormal 90 and 70 kDa heat shock proteins. Leukemia 1996; 10: 994-999.
[23] Wang SX, Chen JX, Yue GX, Bai MH, Kou MJ and Jin ZY. Xiaoyaosan decoction regulates changes in neuropeptide y and leptin receptor in the rat arcuate nucleus after chronic immobilization stress. Evid Based Complement Alternat Med 2012; 2012: 381278.
[24] Chen JX, Li W, Zhao X and Yang JX. Effects of the Chinese traditional prescription Xiaoyaosan decoction on chronic immobilization stress-induced changes in behavior and brain BDNF, TrkB, and NT-3 in rats. Cell Mol Neurobiol 2008; 28: 745-755.
[25] Meng ZZ, Hu JH, Chen JX and Yue GX. Xiaoyaosan decoction, a traditional chinese medicine, inhibits oxidative-stress-induced hippocampus neuron apoptosis in vitro. Evid Based Complement Alternat Med 2012; 2012: 489254.
[26] Meng ZZ, Chen JX, Jiang YM and Zhang HT. Effect of xiaoyaosan decoction on learning and memory deficit in rats induced by chronic immobilization stress. Evid Based Complement Alternat Med 2013; 2013: 297154.
[27] Li XJ, Ma QY, Jiang YM, Bai XH, Yan ZY, Liu Q, Pan QX, Liu YY and Chen JX. Xiaoyaosan exerts anxiolytic-like effects by down-regulating the TNF-alpha/JAK2-STAT3 pathway in the rat hippocampus. Sci Rep 2017; 7: 353.
[28] Kol A, Sukhova GK, Lichtman AH and Libby P. Chlamydial heat shock protein 60 localizes in human atheroma and regulates macrophage tumor necrosis factor-alpha and matrix metalloproteinase expression. Circulation 1998; 98: 300-307.
[29] Zhao ZW, Zhang M, Chen LY, Gong D, Xia XD, Yu XH, Wang SQ, Ou X, Dai XY and Zheng XL. Heat shock protein 70 accelerates atherosclerosis by downregulating the expression of ABCA1 and ABCG1 through the JNK/Elk-1 pathway. Biochimica Et Biophysica Acta 2018; 1863: 806-822.
[30] Raghavan S, Singh NK, Mani AM and Rao GN. Protease-activated receptor 1 inhibits cholesterol efflux and promotes atherogenesis via cullin 3-mediated degradation of the ABCA1 transporter. J Biol Chem 2018; 293: 10574-10589.
[31] Rubic T and Lorenz RL. Downregulated CD36 and oxLDL uptake and stimulated ABCA1/G1 and cholesterol efflux as anti-atherosclerotic mechanisms of interleukin-10. Cardiovasc Res 2006; 69: 527-35.
[32] Naveed P and James Z. Cd36 as a heat shock protein receptor and uses thereof. 2002.
[33] Binder RJ, Vatner R and Srivastava P. The heat-shock protein receptors: some answers and more questions. Tissue Antigens 2004; 64: 442-451.
[34] Asea A. Stress proteins and initiation of immune response: chaperokine activity of hsp72. Exerc Immunol Rev 2005; 11: 34-45.
[35] Deleonpennell KY, Tian Y, Zhang B, Cates CA, Padmanabhan IR, Cannon P, Shah P, Aiyetan P, Halade GV and Ma Y. CD36 is a matrix metalloproteinase-9 substrate that stimulates neutrophil apoptosis and removal during cardiac remodeling. Circ Cardiovasc Genet 2016; 9: 14-25.
[36] Weng CH, Chung FP, Chen YC, Lin SF, Huang PH, Kuo TB, Hsu WH, Su WC, Sung YL, Lin YJ, Chang SL, Lo LW, Yeh HI, Chen YJ, Hong YR, Chen SA, Hu YF. Pleiotropic effects of myocardial MMP-9 inhibition to prevent ventricular arrhythmia. Sci Rep 2016; 6: 38894.
[37] Chen Y, Kennedy DJ, Ramakrishnan DP, Yang M, Huang W, Li Z, Xie Z, Chadwick AC, Sahoo D and Silverstein RL. Oxidized LDL-bound CD36 recruits a Na+/K+-ATPase-Lyn complex in macrophages that promotes atherosclerosis. Sci Signal 2015; 8: ra91.
[38] Park YM. CD36, a scavenger receptor implicated in atherosclerosis. Exp Mol Med 2014; 46: e99.
[39] Wang J, Qi H, Zhang X, Si W, Xu F, Hou T, Zhou H, Wang A, Li G, Liu Y, Fang Y, Piao HL and Liang X. Saikosaponin D from radix bupleuri suppresses triple-negative breast cancer cell growth by targeting beta-catenin signaling. Biomed Pharmacother 2018; 108: 724-733.
[40] Zou C, Tan X, Ye H, Sun Z, Chen S, Liu Q, Xu M, Ye C and Wang A. The hepatoprotective effects of radix bupleuri extracts against d-galactosamine/lipopolysaccharide induced liver injury in hybrid grouper (epinephelus lanceolatus-male symbol × epinephelus fuscoguttatus-female symbol). Fish Shellfish Immunol 2018; 83: 8-17.

[41] Kim YJ, Lee JY, Kim HJ, Kim DH, Lee TH, Kang MS and Park W. Anti-inflammatory effects of angelica sinensis (Oliv.) Diels water extract on RAW 264.7 induced with lipopolysaccharide. Nutrients 2018; 10: 647.

[42] Wu K, Guo C, Yang B, Wu X and Wang W. Antihepatotoxic benefits of poria cocos polysaccharides on acetaminophen-lesioned livers in vivo and in vitro. J Cell Biochem 2018; 120: 7482-7488.

[43] Yang L, Chai CZ, Yan Y, Duan YD, Henz A, Zhang BL, Backlund A and Yu BY. Spasmolytic mechanism of aqueous licorice extract on oxytocin-induced uterine contraction through inhibiting the phosphorylation of heat shock protein 27. Molecules 2017; 22: 1392.

[44] Li N, Liu Q, Li XJ, Bai XH, Jin ZY, Liu YY, Jing YX, Zhao HB. Evaluation of xiaoyaosan in treating rat model of type 2 diabetes associated with depression. China Journal of Traditional Chinese Medicine and Pharmacy 2015.

[45] Chen JL, Tian JS, Zhou YZ, Gao XX and Qin XM. Research progress on antidepressive mechanism of Xiaoyaosan via metabolic network regulation. Chinese Traditional and Herbal Drugs 2014; 45: 2100-2105.

[46] Chien SC, Chang WC, Lin PH, Chang WP, Hsu SC, Chang JC, Wu YC, Pei JK and Lin CH. A Chinese herbal medicine, jia-wei-xiao-yao-san, prevents dimethylnitrosamine-induced hepatic fibrosis in rats. ScientificWorldJournal 2014; 2014: 217525.

[47] Sun HY, Li Q, Liu YY, Wei XH, Pan CS, Fan JY and Han JY. Xiao-yao-san, a Chinese medicine formula, ameliorates chronic unpredictable mild stress induced polycystic ovary in rat. Front Physiol 2017; 8: 729.

[48] Ding XF, Zhao XH, Tao Y, Zhong WC, Fan Q, Diao JX, Liu YL, Chen YY, Chen JX and Lv ZP. Xiao yao san improves depressive-like behaviors in rats with chronic immobilization stress through modulation of locus coeruleus-norepinephrine system. Evid Based Complement Alternat Med 2014; 2014: 605914.

[49] Zhao HB, Jiang YM, Li XJ, Liu YY, Bai XH, Li N, Chen JX, Liu Q, Yan ZY and Zhao FZ. Xiao yao san improves the anxiety-like behaviors of rats induced by chronic immobilization stress: the involvement of the jnk signaling pathway in the hippocampus. Biol Pharm Bull 2017; 40: 187-194.